International Journal of Metallurgical Engineering 2013, 2(2): 221-229
DOI: 10.5923/j.ijmee.20130202.14

Corrosion Characterization of Advanced Steels for Use in the Oil & Gas Industry

Brajendra Mishra

NSF Center for Resource Recovery & Recycling Metallurgical & Materials Engineering Colorado School of Mines, Golden, Colorado, USA

Abstract Drill pipe steels are in contact with CO_2 environments depending on the oil and gas field. These steels have to be resistant to various in-service conditions including aggressive environments containing CO_2, H_2S, O_2, and chlorides, in addition to static and dynamic mechanical stresses. In this respect stress corrosion cracking susceptibility of two grades of drill pipe steel in CO_2 environment have been studied simulating the bottom hole oil and gas well conditions. SSRT results show that SCC susceptibility or loss of ductility changes with temperature and increasing temperature increases the loss of ductility. Optical and electron microscopy shows presence of cracks which are the cause of ductility loss. No $FeCO_3$ is observed below 100 ℃, and density of $FeCO_3$ is higher in grip section than gauge length and this is due to strain disturbance of growth of iron carbonate crystals. Material selection for down hole in CO_2 containing environments needs has been reviewed and probability of SCC occurrence in higher temperatures has been considered. In another critical application, during oil and gas operations, steel pipeline networks are subjected to different corrosion deterioration mechanisms, one of which is microbiologically influenced corrosion (MIC) that results from accelerated deterioration caused by different microbial activities present in hydrocarbon systems. Bacterial adhesion is a detrimental step in the MIC process. The MIC process starts with the attachment of planktonic microorganisms to metal surface that lead to the formation of the biofilm and subsequently results in metal deterioration. The tendency of a bacterium to adhere to the metal surface can be evaluated using thermodynamics approaches via interaction energies. Thermodynamic and surface energy approaches of bacterial adhesion will be reviewed. Also, the factors affecting bacterial adhesion to the metal surface will be presented. In addition, the subsequent physical-chemical interaction between the biofilm and substratumand its implication for MIC in pipeline systems will be discussed.

Keywords Steel, Corrosion, Microbiological, Transport, Sweet Corrosion, Drill Pipe

Sweet Corrosion of Drill Pipe Steels

Corrosion is one of the most important continuous problems of oil and gas production. Several forms of corrosion occur in oilfield and CO_2 corrosion or ―sweet corrosion is one of the most common forms of attack which hydrocarbon production industry is faced with[1]. Drill pipes may be in contact with wet CO_2, H_2S, O_2 and chlorides depending on the oil and gas field. In addition, through drilling action these steels bear static and dynamic mechanical stresses. These steels have to be resistant to these aggressive environments if they are to be viable[2].

Uniform corrosion of steels in aqueous environments containing CO2 has been extensively studied in the literature, and corrosion mechanisms are now very well defined and are already incorporated in corrosion prediction models[3-5]. Also extensive studies have been carried out on the sulfide stress corrosion cracking (SSC) behavior of high strength low alloy (HSLA) carbon steels[6-11]. As the depletion of shallow oil and gas wells forced the industry in moving toward more aggressive and deeper and sourer environments particularly for natural gas extraction, in these environments the probability of SSC occurrence is increased which restricts the utilization of service strength of steels used for casing, tubing, and tool joints. Thus, the need for new grades of HSLA steels having higher mechanical properties with good SSC resistance has grown[6]. It has been mentioned that high tensile strength, high H2S concentrations, low pH, high total pressure, high chloride concentration, lower temperature, high hardness of steel promote SSC and this phenomena is closely related to hydrogen embrittlement as a result of hydrogen ingress into the stresses steel[8,9]. However, there is less information about the stress corrosion cracking (SCC) susceptibility of these steels in environments containing CO_2 as they are subjected to static and dynamic mechanical stresses along with wet CO_2 gas; Perhaps, this phenomena has somewhat been neglected in favor of H2S

* Corresponding author:
bmishra@mines.edu (Brajendra Mishra)
Published online at http://journal.sapub.org/ijmee

corrosion and sulfide stress cracking. Additional research is required to fully define the environmental-material relationship of high strength low alloy drill pipe steels in sweet high temperature, high pressure wells[10].

Intergranular and transgranular stress corrosion cracking of pipeline steels from the soil side have been studied widely[12-16]. Parkins and his research collaborators showed[12] the occurrence of intergranular stress corrosion cracking (IGSCC) due to the presence of relatively concentrated solution of carbonate-bicarbonate. Also their works[13,14] demonstrated happening of transgranular stress corrosion cracking (TGSCC) that produced by a dilute, lower pH solution of carbonate-bicarbonate. Mechanism for IGSCC was described as preferential dissolution at grain boundaries and repeated rupture of the film formed at the crack tip in which crack sides were not attacked. In contrast, TGSCC is associated with dissolution of crack tip and crack sides which accompanied with hydrogen ingress into the steel. Moreover, Colwell et al.[15] have proposed a mechanism for TGSCC of pipe line steels. According to their studies, iron carbonate found in the vicinity of cracks under disbonded coating in the field is formed from bicarbonate which releases its hydrogen. Hydrogen that diffuse into the steel and lead to embrittlement results in TGSCC.

To these ends, stress corrosion cracking susceptibility of API S-135 grade drill pipe steel in CO_2 containing environment was studied, simulating the bottomhole oil and gas well conditions to advance the present understanding of the prediction of materials performance.

1. Experimental Procedure

Slow strain rate test (SSRT) on API S-135 grade drill pipe steel were carried out using a constant extension rate test (CERT) machine that was activated by a ¼ HP 1725 RPM 0-90 VDC permanent magnet motor. The geometry of the SSRT specimens is shown in Figure 1. The composition and mechanical properties of the API S-135 steel are listed in Table 1.

SSRTs were performed to understand the effect of temperature on the SCC susceptibility of API S-135 drill pipe steel. Experiments were performed in a one liter Inconel 600 autoclave at different temperatures in CO_2 saturated deionized and ultra filtered (DI.U.F) water. The SSRTs were carried out in air and in the corrosive solution at strain rate of $1x\ 10^{-6}\ s^{-1}$ at 25, 50, 75, 100, 125, 150, and 175℃. Every experiment was repeated twice and three times in some cases. To perform the experiments in corrosive environment, 850 ml DI.U.F water was poured inside the autoclave and after tightening the autoclave; CO_2 was purged one hour to deaerate and saturate the solution and finally heated to the desired test temperature using a proportional integral derivative (PID) temperature controller. As soon as temperature reached the desired temperature SSRT was started. To calculate the SCC susceptibility of S-135 drill pipe steel at different temperatures the plastic strain to failure (EP) and reduction in area (RA) were determined from the stress-strain curve and broken specimens respectively. Plastic strain to failure was obtained by subtracting the elastic strain at failure from the total strain at failure. As aforementioned CERT apparatus measures the crosshead displacement instead of the direct gauge section measurement, to avoid displacement contribution from shoulders of test specimens and from the load train this parameter is used. Reduction in area was measured from the difference between the initial area of specimens at the middle of gauge length and reduced area after fracture which was measured using optical microscopy. The ratio of Plastic strain to failure and reduction in area at corrosive environment (EPE and RAE) to inert (air) environment (EPA and RAA) determined as ductility ratio (EPR% and RAR%) which is a measure of SCC susceptibility. The closer the ductility ratio is to 100, the higher is the resistance to environmental cracking[16].

Phase analysis of corrosion products was obtained using X-ray diffraction (XRD) method with a Philips PW 3040/60 spectrometer using Cu K αradiation. FEI Quanta 600i scanning electron microscopy (SEM) was used to study the morphology of corrosion product layer.

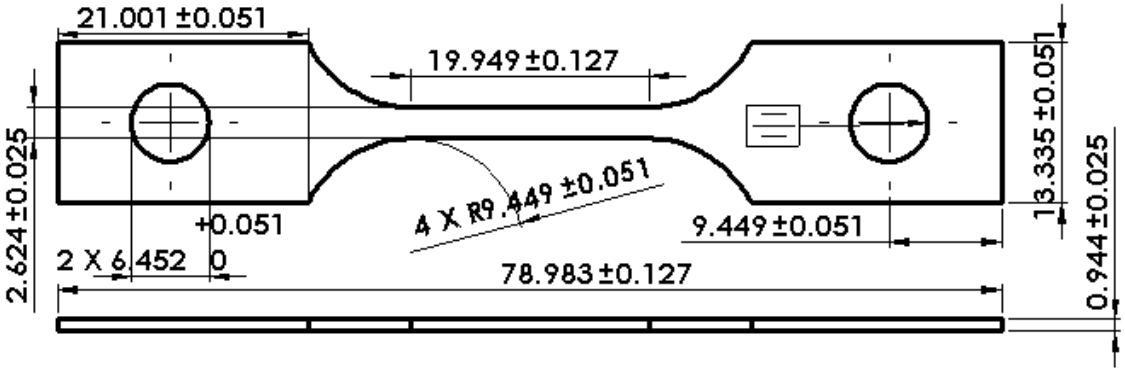

Figure 1. Pin loaded tensile test specimen geometry used for slow strain rate testing

Table 1. Mechanical properties & chemical composition of drill pipe steels[2]

	Yield Strength					Tensile Strength				
Grade	Min		Max			Min				
	ps		MPa	psi		MPa	psi		MPa	
G-105	105,000		724	135,000		931	115,000		793	
S-135	135,000		931	165,000		1138	145,000		1000	
Element	**C**	**Mn**	**Si**	**Ni**	**Cr**	**Mo**	**Al**	**P**	**S**	**Fe**
G-105	0.27	1.33	0.31	0.03	0.92	0.28	0.11	0.013	0.006	Bal.
S-135	0.25	0.8	0.27	0.02	1.26	0.69	0.03	0.008	0.002	Bal.

2. Results and Discussion

(i) *SCC Susceptibility of S-135 Grade Drill Pipe Steel at Different Temperatures*

Ductility ratios (EPR% and RAR%) curves for API S-135 grade drill pipe steel measured in SSRT method in DI.U.F. water saturated with CO_2 are shown in Figures 2 and 3. The test results are summarized in Table 2.

As Figures 2 and 3 show, the ductility of the specimens decreased in solution due to corrosivity at 25, 50, and 75℃. An increase from 75 to 100℃ for EPR was observed but again increasing temperature from 125 to 175℃ caused reduction in ductility ratios. The first decrease is attributed to the increase in corrosion rate and reduction in the cross section of tensile specimen. Since corrosivity and temperature both playing competing role on ductility ratio, at 100^0C the influence of temperature becomes predominant and this governance cause an increase in ductility ratio. Ductility ratios in Figures 2 and 3 for 100℃ show that longitudinal strain is more significant than transverse strain. The second decrease from 125 to 175℃ is due to the formation of protective corrosion products which passivate the steel from further uniform corrosion and leads to localized corrosion, initiation of cracks and finally stress corrosion cracking. SEM studies of fracture morphology of the specimens were carried out to investigate this behavior. Figure 4 shows cracking and fracture morphology (side view) of S-135 grade drill pipe steel tested in CO2 saturated DI water at different temperatures with a strain rate of 10^{-6} s^{-1}. Results indicated that up to 75℃ no crack was observed on the specimen, but at 100℃ cracks are developed only in necking area and extended to the gauge length at 125, 150, and 175℃. In addition, increasing temperature increased the depth of the cracks as well as cracks size. In the next phase of this study the crack formation mechanism and type of stress corrosion cracking (IGSCC or TGSCC) will be investigated and published in a little while.

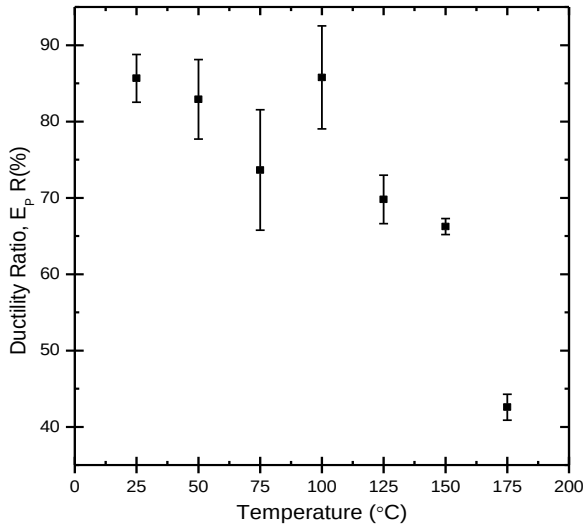

Figure 2. Ductility ratio, E_PR, in the CO_2 saturated solution and air for the S-135 grade drill pipe steel at different temperatures & 10^{-6} s^{-1} strain rate

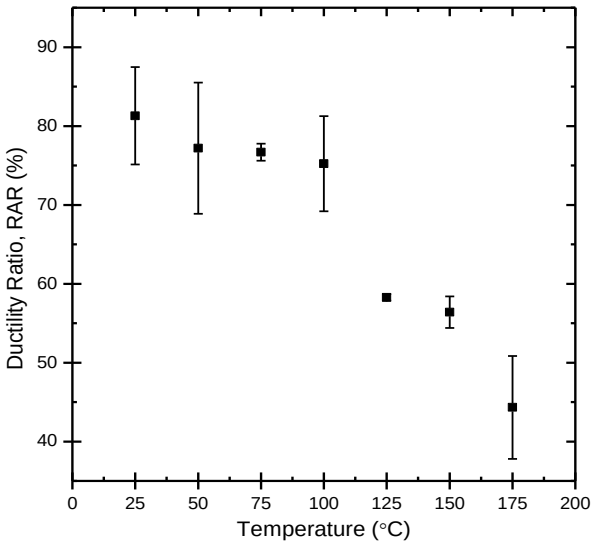

Figure 3. Ductility ratio, RAR, in the CO_2 saturated solution and for the S-135 grade drill pipe steel at different temperatures and 10^{-6} s^{-1} strain rate

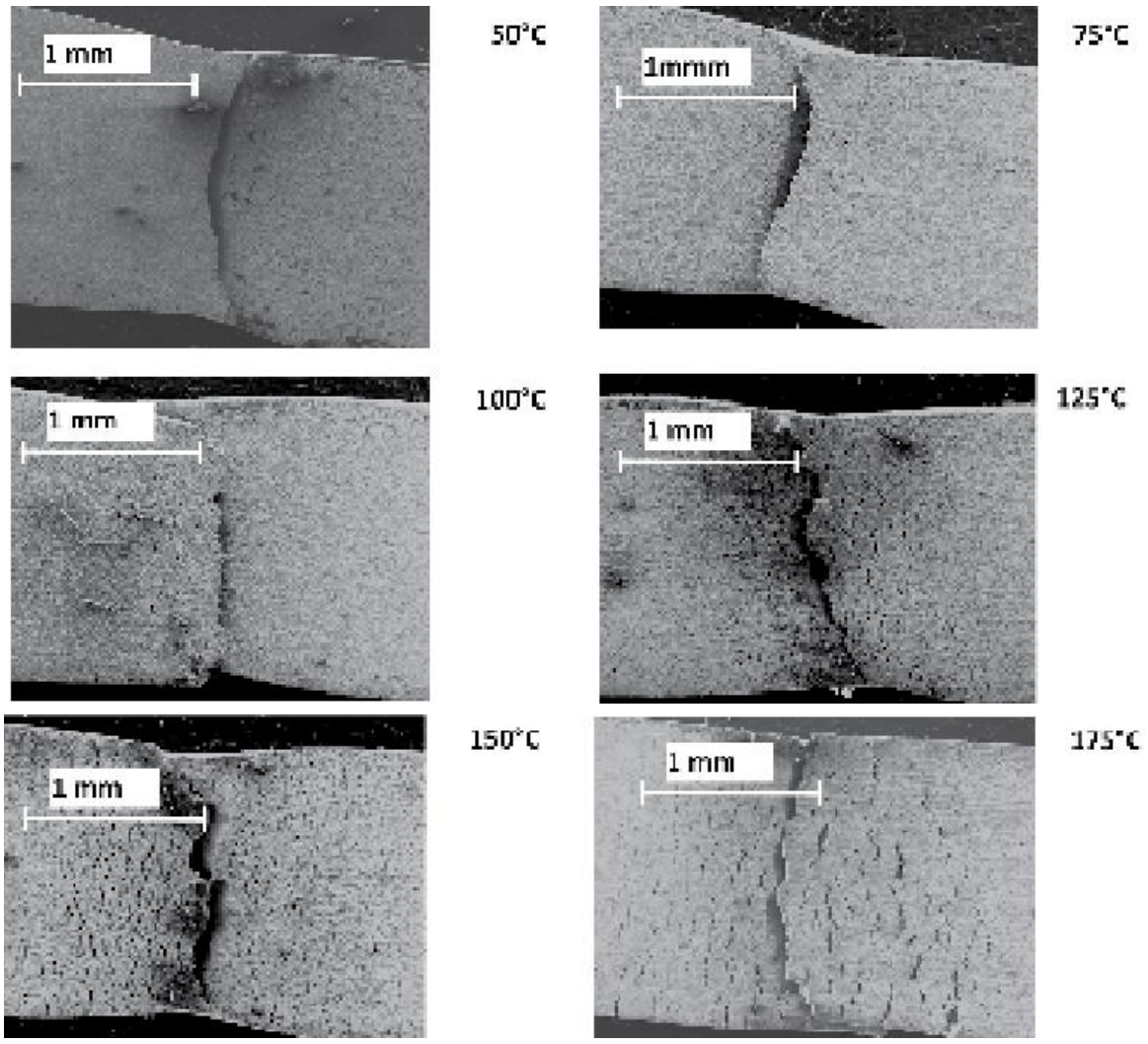

Figure 4. *F*racture morphologies of S-135 grade drill pipe steel tested in CO_2 saturated DI water at different temperatures with a strain rate of 10^{-6} s^{-1}

Microbiologically Induced Corrosion of Pipeline Steels

Microorganisms that are present in oil reservoirs are able to induce localized changes in the aqueous environment (e.g., alter the concentration of the electrolyte components pH and oxygen concentration) leading to localized corrosion known as microbiologically influenced corrosion (MIC). Microbial activities are responsible for approximately 20% of the total corrosion cost in the oil and gas industry, of which a significant part is due to anaerobic corrosion influenced by sulfate reducing bacteria (SRB) and aerobic corrosion influenced by iron-reducing and oxidizing bacteria (IRB/IOB)[17]. The metabolic by-products of these microorganisms found in biofilms on steel surfaces affect the kinetics of cathodic and/or anodic reactions. Moreover, these metabolic activities can considerably modify the chemistry of any protective layers, leading to either acceleration or inhibition of localized corrosion[17].

The objective of this study is to investigate the impact of environmental aerobic bacteria (cultivated from oil field samples rather than obtained from a culture collection) on the corrosion behavior of low alloy high strength (API 5L X80) linepipe steel. The IRB consortium used in this study was cultivated from a sour oil well in Louisiana, USA.

3. Experimental Methods

3.1. Organisms and Testing Medium

The IRB consortium used in this study was cultivated from water samples obtained from a sour oil well located in Louisiana, USA. The water samples were collected and bottled at the wellhead from an approximate depth of 2200 ft. as described by NACE Standard TM0194[18]. For IRB isolation, one milliliter of the water sample was transferred to a 250 ml of Erlenmeyer flask containing 100 ml of LB broth medium. The LB medium was composed of tryptone (10 g), sodium chloride (10 g), and yeast extract (5.0 g) added to one liter of distilled water. The pH of the medium was adjusted to 7.2 using 5M sodium hydroxide and autoclaved for 20 min. The bacteria were incubated at 30 ^{o}C in a rotary shaker at 150 rpm until turbid growth was observed.

3.2. Identification of the Iron-reducing Consortium

DNA was extracted from cultivars using the MoBio Powersoil DNA extraction kit. 16S rRNA gene amplification was carried out using the 'universal' polymerase chain reaction (PCR) primers 515F and 1391R. PCR, cloning and transformation were then carried out as described by Sahl et al.[19]. Unique restriction fragment length polymorphisms (RFLP) were sequenced on an ABI 3730 DNA sequencer at Davis Sequencing, Inc. (Davis, CA). Sanger reads were called with PHRED via Xplorseq[20]. Sequences were compared to the GenBank database via BLAST (http://blast.ncbi.nlm.nih.gov/Blast.cgi).

3.3. Specimen Preparation

Steel coupons (10 mm x 10 mm x 5 mm) were cut from a 6-inch (12.5 mm) section of API-5L X52 carbon steel pipe with chemical composition (wt.%): 0.07C, 1.05Mn, 0.008S, 0.03Cr, 0.008P and 0.195Si. The coupons were embedded in a mold of non-conducting epoxy resin, leaving an exposed area of 100 mm^2. For electrical connection, a copper wire was soldered at the rear of the coupons. The coupons were polished with progressively finer sand paper to a final grit size of 600 microns. After polishing, the coupons were rinsed with distilled water, ultrasonically degreased in 100% acetone followed by 100% ethanol and sterilized by exposure to 100% ethanol for 24 hours.

3.4. Electrochemical Tests and Surface Analysis of the Coupons Exposed to IRB

The electrochemical measurements and subsequent surface analysis were performed per the procedure described by Al-Abbas et al.[21] elsewhere.

4. Results and Discussion

4.1. Identification of the Iron-reducing Consortium

16S rRNA gene analysis indicated that the mixed bacterial culture consortium contained two phylotypes: members of the *Proteobacteria* (*Shewanella oneidensis sp.*) and *Firmicutes* (*Brevibacillus sp.*). *Shewanella oneidensis* are facultative anaerobic iron-reducing bacteria that are capable of diverse metabolisms. They are able to reduce ferric iron and sulfite, oxidize hydrogen gas, and produce sulfide. It has been reported that these bacteria might be involved in biocorrosion whereas some studies suggest that *Shewanella oneidensis* may have an inhibitory effect towards corrosion[22]. *Brevibacillus* are aerobic spore-forming microbes. They have the ability to degrade hydrocarbons and plastics. They were used to treat part of the Daqing oil field, in which the oil production increased by 165% for about 200 days[23].

4.2. Morphology and Composition of Interfacial Surfaces

The morphology observations of corrosion products of API X52 carbon steel exposed to sterilized control medium (abiotic) and inoculated medium (biotic) are shown in Figure 5A and 5B, respectively. For the abiotic system, there is one homogenous layer of corrosion product (Figure 5A) formed on the surface with some deposited salt crystals. Quantitative EDS analysis, spectra not shown here, revealed peaks for oxygen, iron, chloride sodium and carbon that accumulated from the growth medium. The EDS analysis suggests that the corrosion layer is composed of iron oxides mixed with sodium chlorides and organic compounds. There is significant difference in the characteristics of the layer that developed in the presence of the IRB microbial consortium (biotic) as shown in Figure 5B. The significant amount of products observed in the biotic system is most likely due to the production of a biofilm matrix. Figure 5C displays higher magnifications of the biofilm structure that confirms bacterial attachment to the metal surface. In the case of the biotic condition, the EDS analysis revealed peaks for nitrogen and phosphorus in addition to oxygen, iron, chloride, sodium and carbon. The presence of the nitrogen and phosphorus may be due to the microbial production of extracellular polymer substance (EPS)[24].

IRB cells attached to the substrate produce EPS, which results in biofilm formation. The biofilm has a heterogeneous morphology and thickness as shown in Figure 5B. The rod-shaped bacteria occupied a small volume fraction as compared to the precipitated corrosion products and EPS. The EPS and corrosion products usually occupy 75-95 % of biofilm volume, while 5-25% is occupied by the cells[25].

The coupons immersed in the abiotic medium exhibit aggressive and elongated pitting (Figure 5C) in comparison with the biotic coupons that still show the polishing marks along with shallow pitting (Figure 5D). The protective effects of the biofilm in the case of biotic condition are attributed to the reduction of ferric ions to ferrous ions and increased consumption of oxygen by *Shewanella oneidensis sp* respiration. Dubiel et al.[26] reported that *Shewanella oneidensis sp.* inhibit corrosion on stainless steel surfaces in a medium containing yeast extract and peptone. Interestingly, it has been proposed that *Shewanella oneidensis sp.* be used to control corrosion in pipeline systems. *Shewanella oneidensis sp.* may colonize the metal surface and consume oxygen molecules adjacent to the metal surface by aerobic respiration. As oxygen is depleted, the bacteria turn to Fe^{3+} anaerobic respiration and produced Fe^{2+} ions diffuse into the bulk fluid. In static environments, this process will create a chemical shield that reduces oxygen diffusion, which in turn, inhibits the cathodic reaction due to lower oxygen availability. By electrochemical reaction Fe^{2+} is oxidized to Fe^{3+} and again reduced by bacterial respiration. Consequently, corrosion will be inhibited[27].

4.3. Polarization Resistance/ Corrosion Rate

The polarization resistance (Rp) variations for the biotic and abiotic systems are shown in Figure 6A. The LPR as a function of time data revealed that in the biotic medium a substantial increase of polarization resistance (Rp) to 7000 $\Omega.cm^2$ was followed by a decrease to 5000 $\Omega.cm^2$ at 100 hours, which then remained stable at approximately 6500 $\Omega.cm^2$ throughout the period of exposure. The polarization resistance is inversely proportional to the corrosion current, which means lower corrosion rate at higher Rp resistance. This trend confirms the corrosion inhibition effects induced by the activity of the bacterial consortium. On the other hand, in the abiotic medium, the Rp trend remained more or less steady at approximately 1500 $\Omega.cm^2$ over the entire period. When comparing the two Rp trends for the biotic and abiotic medium, the Rp values for the abiotic medium are significantly lower than those for the biotic medium. This observation suggests that the corrosion rate is substantially higher in the abiotic medium. The corrosion rate plots over time for the biotic and abiotic systems are shown in Figure 6B. The corrosion rate for the abiotic medium reached a maximum value of 20 mpy after 200 hours whereas the corrosion rate for the biotic system was around 2 mpy over the experimental period.

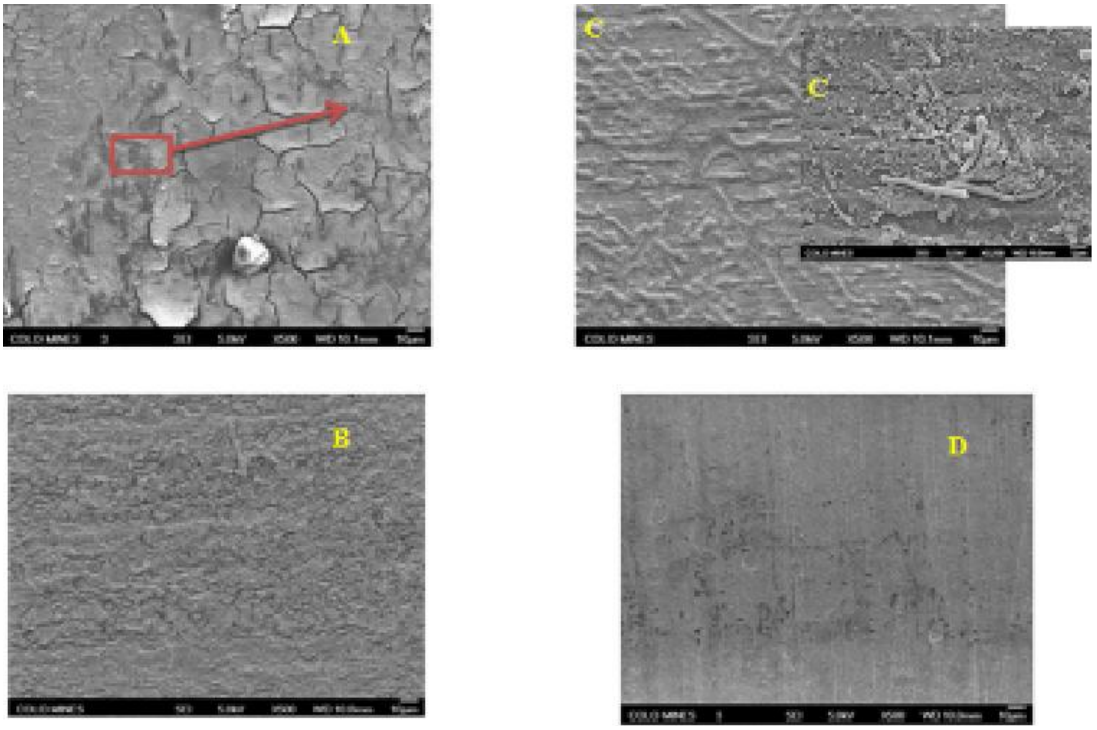

Figure 5. FESEM for the API 5L X52 surface: (A) FESEM image of carbon steel exposed to sterile LB medium nutrients, at 500X. (B). FESEM Image of carbon steel exposed to LB medium inoculated with IRB at 500X. (C) Higher magnification (X6500.) of image (A) shows the bacteria cells. (D) Clean metallic surface removed from biotic system at 500X. (F) Clean metallic surface removed from biotic system

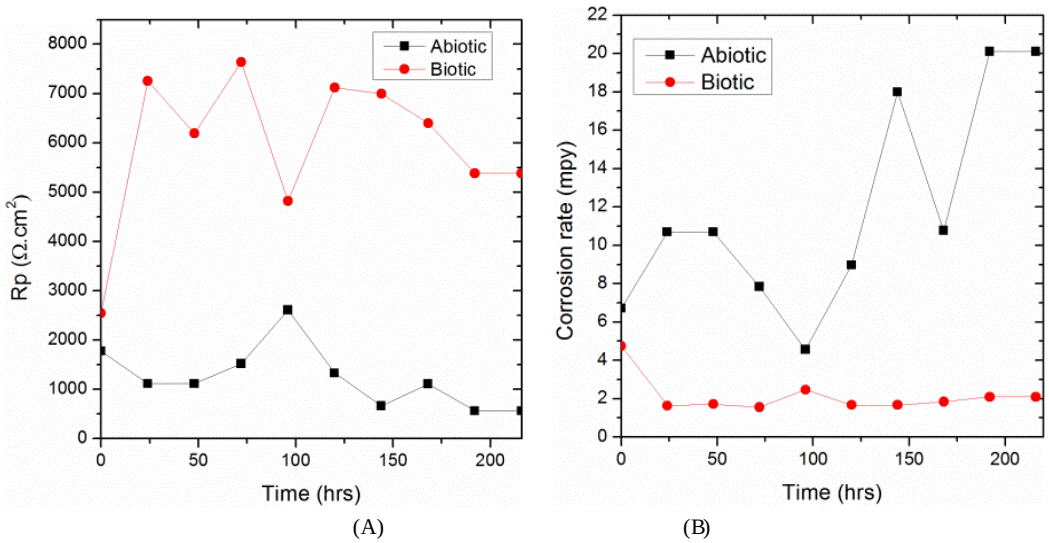

(A) (B)

Figure 6. (A) Polarization resistance, (B) Corrosion rates variations for both biotic and abiotic media

Both Rp and corrosion rate data confirm the corrosion inhibition properties of the bacterial consortium. This inhibition cannot be explained by a single mechanism[27]. It might be attributed to the oxygen depletion induced by bacterial respiration[27]. The change in oxygen concentration caused by microbial respiration can decrease the cathodic reaction rate by reducing the amount of reactants available for the cathodic reaction. A similar inhibitory mechanism for steel in the presence of two marine isolates in saline media was reported by Pedersen and Hermansson[28]. It is also possible that the biofilm developed by the bacteria contributes to the low corrosion in the biotic medium. There have been a few reports of corrosion inhibition in the presence of biofilms[17]. Biofilms and attached cells may form a diffusion barrier hindering the reactants diffusion to and from the metal surface[29]. Another mechanism that might be responsible for the corrosion inhibition is related to the generation of a cathodic protection current by the bacterial consortium. It was reported that *Shewanella oneidensis sp.* produced electrically conductive pilus-like appendages called bacterial nanowires that can transfer electrons to the electrode. The capability of *Shewanella oneidensis sp.* to transfer electrons from organic sources to electrodes without intervening catalysts serves as the basis for electricity production in microbial fuel cells[30]. Moreover, *Brevibacillus sp.* has been investigated in microbial fuel cells for their capacity to generate electrons[31]. Interestingly, previous studies show the capacity of *Brevibacillus sp.* to produce electricity increases in the presence of *Pseudomonas sp.* due to the metabolites produced by *Pseudomonas sp.*, which enable *Brevibacillus sp.* to achieve extracellular electron transfer[31]. Based on these facts, it is possible, that *Brevibacillus sp.* and *Shewanella oneidensis sp.*, through their complimentary metabolisms, produce cathodic currents that result in corrosion inhibition. The increase in corrosion rate noticed in the abiotic medium is possibly due to the effect of a formation of a mixed non-protective layer of sodium chloride, iron oxides and carbon-based compounds on the electrode surface[25].

4.4. Electrical Impedance Spectroscopy (EIS) Results

Figure 7A displays the Nyquist plots for the carbon steel coupon exposed to the abiotic medium over time. The steady state was reached at 120 hours. At low frequencies (LF), shown in Figure 7A, the magnitude of the capacitive loop represented by the semicircle diameter decreased with time. These LF magnitudes represent the change in charge transfer resistance (Rct) that describes the evolution of the anodic reaction that is controlled by charge transfer processes[25]. The decrease of Rct with time indicates an increase in corrosion rate, possibly due to the effect of a formation of a mixed layer of sodium chloride, sulfide, potassium and carbon-based compounds on the electrode surface. Moreover the presence of oxygen in the system enhances the cathodic reactions that drive the anodic dissolution of the metal[25]. The formation of a corrosion product layer was confirmed by the phase angle spectra (Figure 7B) that shows two time constants at 10 Hz and 0.1 Hz medium frequencies, as indicated by the arrows in Figure 3B.

When the carbon steel was exposed to the inoculated culture medium (biotic), the EIS spectra varied significantly with exposure time as shown in Figure 8A. The low frequency (LF) magnitude, represented by the semicircle diameter, significantly increased with time indicating a decrease in corrosion rate and increase in charge transfer resistance (Rct) as supported by Figure 8A.

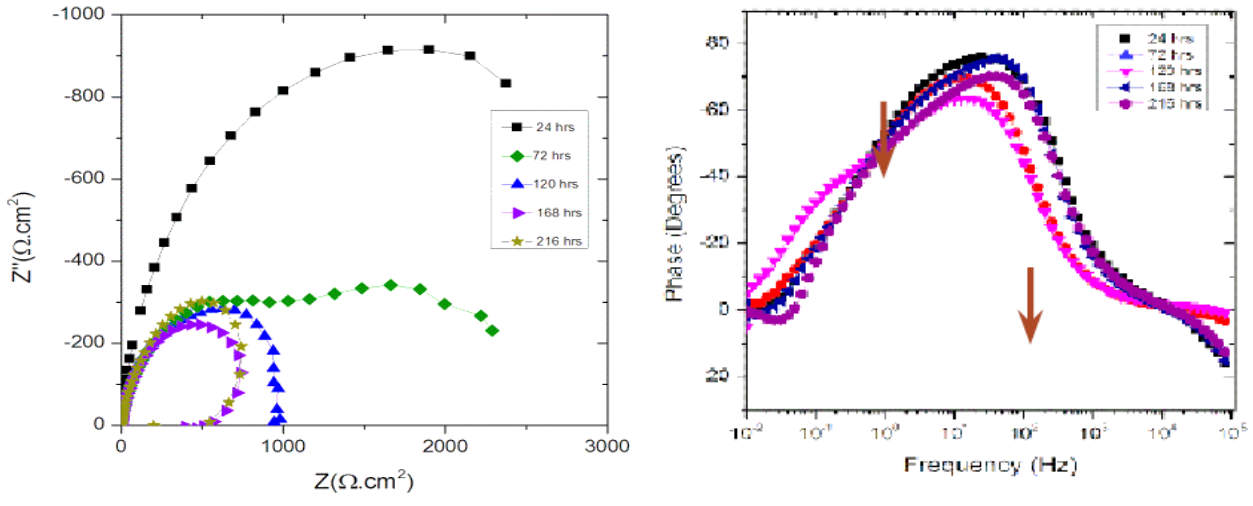

(A) (B)

Figure 7. EIS date for abiotic culture medium; (A) Nyquist Plots (B) Phase angle plots

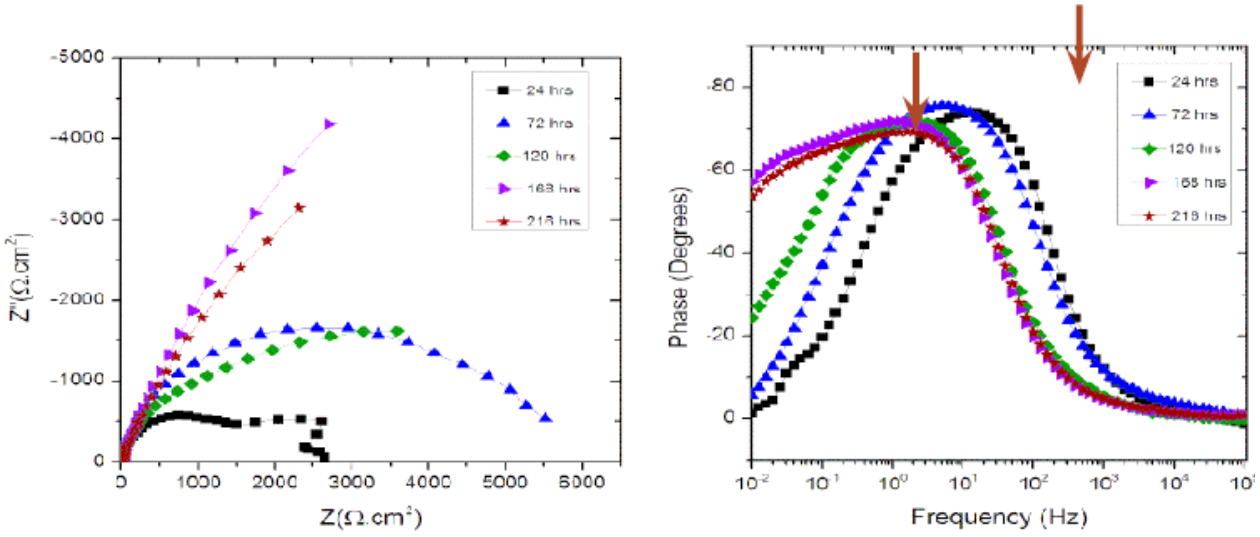

(A) (B)

Figure 8. EIS date for inoculated biotic medium; (A) Nyquist Plots (B) Phase angle plots

For the first 72 hours, the medium frequency (10 Hz) response presented in the phase diagram in Figure 8A shows one time constant that indicates an activation control process. This behavior is attributed to the formation of an unstable conditioning layer based on a mixture of inorganic/ organic compounds[21]. However, when stable biofilm formation was achieved at 120 hours and when steady state is reached, mass transfer limitations overcome the interfacial activation, which is reflected in a change from a semicircle behavior to a straight line shown in Figure 8A. It is speculated that the formation of an adherent biofilm influenced the mass transfer processes in the electrochemical cell[25]. The formation of biofilm is confirmed by the two time constants indicated by arrows in Figure 8B. The EIS spectra affirm the inhibitory effect of the bacterial activities and subsequent biofilm formation described in the previous sections of this paper. Potentially the IRB consortium could be use as a strategy to combat corrosion especially in aerobic environment.

5. Conclusions

• Fracture surface studies revealed the occurrence of stress corrosion cracks when conducting SSRTs on API S-135 grade drill pipe steel in CO_2 saturated environment at temperatures above 100℃.

• SEM and XRD studies showed the formation of protective rhombohedral $FeCO_3$ at 100 ℃ and above temperatures on the surface passivating the steel which later leads to localized corrosion and initiation of cracks. Some of the cracks formed on the surface may become inactive, but some may be reactivated by coalescence with later nucleated cracks and perhaps by stress condition variation.

• At lower temperatures cracks did not develop in gauge length meaning that protective corrosion products were not formed on the surface and uniform corrosion of steel occurred.

• SCC occurs in the absence of uniform corrosion. Creation of favorite condition for protective scale formation at 100℃ and above prevents uniform corrosion which leads to initiation of cracks from susceptible areas. Increasing temperature increases the kinetics of reactions and faster initiation and propagation and higher loss of ductility.

• In the microbiologically influenced corrosion (MIC) study of API 5L grade X52 carbon steel coupons by an iron-reducing consortium cultivated from a sour oil well produced water was investigated. Interestingly, IRB metabolic reactions and biofilm formation inhibit the corrosion process. The maximum corrosion rate in the biotic system was 2 mpy while it was 20 mpy in the abiotic solution. The corrosion inhibition was attributed to oxygen depletion induced by IRB bacteria respiration and the protective affect of the biofilm that formed on the metal surface.

REFERENCES

[1] M. B. Kermani, and A. Morshed, ―Carbon dioxide corrosion in oil and gas production-A Compendium, Corrosion 59, 659 (2003)

[2] J. Mougin, M.S. Cayard, R.D. Kane, B. Ghys, and C.Pichard, ―Sulfide stress cracking and corrosion fatigue of steels dedicated to bottom hole assembly components, NACE, paper 05085, 2005.

[3] B. Mishra, S. Al-Hassan, D.L. Olson, and M.M. Salama, ―Development of a predictive model for activation-controlled corrosion of steel in solutions containing carbon dioxide, Corrosion, Corrosion 53, 852 (1997)

[4] B. Mishra, D.L. Olson, S. Al-Hassan, and M.M. Salama, ―Effect of Microstructure on Corrosion of Steels in Aqueous Solutions Containing CO2 Corrosion, 54, 480

(1998).

[5] C. De Dewaard and D. E. Milliams, ―Carbonic Acid Corrosion of Steel, Corrosion, 31, 177 (1975).

[6] J. C. Charbonnier, H. Margot-Marette, A. M. Brass, and M. Aucouturier, ―Sulfide Stress Cracking of High Strength Modified Cr-Mo Steels, Metallurgical Transaction A, Vol. 16A, May 1985, p 935.

[7] R. Brett Chandler, Michael J. Jellison, James W. Skogsberg, Tom Moore, ―Advanced drill string metallurgy provides enabling technology for critical sour drilling, Paper No. 02056, NACE 2002.

[8] R. D. Kane and M. S. Cayard, ―Roles of H2S in the behavior of engineering alloys: A review of literature and experience, Paper No. 274 NACE 1998.

[9] M. Elboujdaini and R. V. Revie, ―Metallurgical factors in stress corrosion cracking (SCC) and hydrogen induced cracking (HIC), J Solid State Electrochem (2009) 13: 1091-1099.

[10] A Robert Mack, ―Stress corrosion cracking of high strength steels in aqueous solutions containing CO2- effects of yield strength, dissolved oxygen, and temperature, NACE, paper 01076, 2001.

[11] Byoung-Ho Choi and Alexander Chudnovsky, ―Observation and modeling of stress corrosion cracking in high pressure gas pipe steel, Metallurgical and Materials Transaction A, 13 August 2010.

[12] R. N. Parkins, ―Mechanistic Aspect of intergranular stress corrosion cracking of ferritic steels, Corrosion, 52, 363 (1996).

[13] R. N. Parkins, W. K. Blanchard Jr., and B.S. Delanty, ―Transgranular stress corrosion cracking of high-pressure pipelines in contact with solutions of near neutral pH, Corrosion, Vol. **50**, 395, (1994).

[14] J. A. Colwell, B. N. Leis, P. M. Singh, ―Recent developments in characterizing the mechanism of near neutral pH SCC, NACE, paper 05161, 2005.

[15] B. Gu, W. Z. Yu, J. L. Luo, X. Mao, ―Transgranular stress corrosion cracking of X-80 and X-52 pipeline steels in dilute aqueous solution with near-neutral pH, Corrosion, Vol. 55, No. 3, p 312.

[16] National Association of Corrosion Engineers standard ―Standard Test Method Slow Strain Rate Test Method for Screening Corrosion-Resistant Alloys (CRAs) for Stress Corrosion Cracking in Sour Oilfield Service, TM0198-2004.

[17] B.J. Little and J.S. Lee. 2007. *Microbiologically Influenced Corrosion*. John Wiley & Sons Inc., Hoboken, NJ, USA; pp: 1-50.

[18] NACE Standard TM0194. 2004. "Field Monitoring of Bacterial Growth in Oil and Gas Systems". Published by NACE, Houston, Texas.

[19] W. Sahl, F. Nathaniel, H.J. Kirk, W. David, W.C. Stone and J. R. Spear. 2010. "Novel Microbial Diversity Retrieved by Autonomous Robotic Exploration of the World's Deepest Vertical Phreatic Sinkhole" *Astrobiology*, 10(2):201–13.

[20] D. Frank, 2008. XplorSeq: a software environment for integrated management and phylogenetic analysis of metagenomic sequence data. *BMC Bioinformatics* 9: 9–420.

[21] F.M. Alabbas, A.B. Gavanluei and J.R. Spear et al., 2011. "Effects of Sulfate Reducing Bacteria on the Corrosion of X-65 Pipeline Carbon Steel" Paper # C2012–0001140, Proceeding NACE 2012 Conference.

[22] M.T. Lutterbach, L. Contador, A. Oliveira and M. Galvão . 2009. "Iron Sulfide Production by *Shewanella* Strain Isolated From Black Powder" Paper # 09391, Proceeding NACE 2009 Conference.

[23] N. Youssef, M.S. Elshahed and M.J. McInerney.2009. "Microbial Processes in Oil Fields: Culprits, Problems, and Opportunities", *Adv. Appl. Microbiol.* 66:141–251.

[24] C. Shobhana, G. Gunasekaran and Pradeep Kumar. 2005. "Corrosion Inhibition of Mild Steel by Aerobic Biofilm" *Electrochimica Acta*, 50 (24):4655–4665.

[25] H. Castaneda and X.D. Benetton. 2008. "SRB-Biofilm Influenced in Active Corrosion Sites Formed at the Steel-Electrolyte Interface When Exposed to Artificial Seawater Conditions" *Corrosion Science* 50:1169–1183.

[26] M. Dubiel, C.H. Hsu, C.C. Chien, F. Mansfield and D.K. Newman. 2002. "Microbial Iron Respiration Can Protect Steel From Corrosion" *Applied and Environmental Microbiology* 68, 1440–1445.

[27] L.K.Herrera and H.A. Videla. 2009. "Role of Iron-Reducing Bacteria in Corrosion and Protection of Carbon Steel" *International Biodeterioration & Biodegradation* 63: 891–895.

[28] A. Pedersen, M. Hermansson.1991. "Inhibition of Metal Corrosion by Bacteria" *Biofouling* 3:1–11.

[29] H.A. Videla and L. K. Herrera. 2009." Understanding Microbial Inhibition of Corrosion. A Comprehensive Overview" *International Biodeterioration & Biodegradation* 63:896–900.

[30] Y.A. Gorby, Y. Svetlana and McLean J. S. et al. 2006. "Electrically Conductive Bacterial Nanowires Produced by *Shewanella oneidensis* Strain MR-1and Other Microorganisms" *PNAS* 103: 11358-11363.

[31] T.H. Pham, Boon N. and Aelterman P. et al. 2008. "Metabolites Produced by *Pseudomonas sp.* Enable a Gram Positive Bacterium to Achieve Extracellular Electron Transfer" *Appl Microbiol Biotechnol* 77:1119–1129.